Overexpressing NRT2.7 induces nitrate export from the vacuole and increases growth of Arabidopsis

Patrick Armengaud[1*], Alexis De Angeli[2**], Patrick Berquin[1], Virginie Bréhaut[1], Mickaël Durand[1***], Françoise Daniel-Vedele[1], Anne Krapp[1#] and Sophie Filleur[2,3#]

[1] Université Paris-Saclay, INRAE, AgroParisTech, Institut Jean-Pierre Bourgin for Plant Sciences (IJPB), 78000, Versailles, France;
[2] Université Paris-Saclay, CEA, CNRS, Institute for Integrative Biology of the Cell (I2BC), 91198, Gif-sur-Yvette, France;
[3] Université Paris Cité, UFR Sciences du Vivant, 35 rue Hélène Brion, F-75205 Paris Cedex 13, France.

*Present address: INRIA Rocquencourt, Domaine de Voluceau, Rocquencourt - BP105, 78153 Le Chesnay Cedex, France
**Present address: Institute for Plant Sciences of Montpellier (IPSiM), Université de Montpellier, CNRS, INRAE, Institut Agro, Montpellier, 34060, France.
***Present address: Biomolécules et Biotechnologies Végétales, EA2106, Université de Tours, Tours, France

Email addresses of the authors :
Patrick Armengaud : patrick.armengaud@inria.fr
Alexis De Angeli : alexis.deangeli@cnrs.fr
Patrick Berquin : patrick.berquin@inrae.fr
Virginie Bréhaut : virginie.brehaut@inrae.fr
Mickaël Durand : midurand@univ-tours.fr
Françoise Daniel-Vedele : fravedele@yahoo.fr
Anne Krapp (# co-corresponding authors) : anne.krapp@inrae.fr
Sophie Filleur (# co-corresponding authors) : sophie.filleur@i2bc.paris-saclay.fr

Date of submission: 13/02/2025

Number of tables: 0

Number of figures: 5

Word count: 5230

Number of supplemental figures: 5

Number of supplementary tables: 1

Running title: Physiological impact of vacuolar nitrate transport

48

49 **Highlight :**

50 The overexpression of the nitrate transporter NRT2.7 stimulates growth by increasing
51 the export of nitrate from the vacuole, the main cell compartment for nitrate storage.

52

53 ## Abstract

54 Nitrogen nutrition is essential for crop yield but applying fertilizers has
55 detrimental effects on the environment. Compartmenting nitrate into vacuoles is one of
56 the options to develop Nitrogen-efficient crop adapted to less fertilizers. Only few
57 proteins involved in nitrate transport on the tonoplast have been identified. CLCa is the
58 major transporter involved in nitrate storage in Arabidopsis but it can also facilitate
59 nitrate remobilization from the vacuole in guard cells. Several other nitrate transporters
60 amongst NRT2.7 have been localized in this membrane. The transport mechanism of
61 NRT2.7 has not yet been defined as this protein is present mainly in seed cells that
62 are not easily amenable for electrophysiology analysis. Here, we investigated NRT2.7
63 function through its ectopic overexpression in a *clca* knock-out mutant. Although the
64 growth diminution of *clca* on nitrogen sufficient medium was complemented, nitrate
65 homeostasis was not restored by NRT2.7 activity. Moreover, NRT2.7 ectopic
66 overexpression in wild-type background (WT) increased growth under limiting nitrogen
67 supply, suggesting that NRT2.7 stimulates nitrate efflux from vacuoles. This hypothesis
68 was demonstrated by electrophysiological nitrate flux measurements on isolated
69 vacuoles. This discovery of NRT2.7 function and more largely the coupling of vacuolar
70 nitrate fluxes with growth under low nitrate supply, will enable new strategies for
71 engineering better NUE for a more sustainable agriculture.

72

73 **Keywords:** Arabidopsis, Electrophysiology, Nitrate homeostasis, Nitrate transporter,
74 NRT, vacuolar membrane

75

76

77 **Abbreviations:**

78 CaMV: Cauliflower Mosaic Virus

79 CLC: ChLoride Channel

80 KO: Knock-out

81 N: Nitrogen

82 NPF: Nitrate transporter 1/Peptide transporter Family

83 NRT2: High affinity Nitrate transporter

84 NUE: Nitrogen Use Efficiency

85 WS: Wassilewskija Arabidopsis accession

86

87 ## Introduction

88 Nitrogen (N) is an essential macronutrient acquired by plants from the soil or the air to
89 synthesize amino acids, nucleotides and proteins. Most cultivated plant species rely
90 on soil soluble ammonium and nitrate, the latter being the most abundant oxidized form
91 of nitrogen found in temperate agricultural soils in amounts ranging from 0.1 to 10 mM
92 (Miller *et al.*, 2007). The effect of N supply on plant growth has long been evidenced
93 and this nutritional benefit was the basis of the fertilizer-driven yield increases. Crops
94 are therefore abundantly provided with nitrogen fertilizers to insure best yield. This
95 practice is at high economic and ecological costs since it has been shown that plants
96 use only 25 to 50 % of nitrogen applied in the field (Cassman *et al.*, 2002). Because of
97 both nitrate mobility and soil structure, nitrate leaks from the field, contaminates water
98 effluents and stimulates growth of algae and microorganisms leading to ecological
99 problems such as river eutrophication (Howarth and Marino, 2006). To avoid these
100 problems and move toward a more sustainable agriculture, one means is to reduce
101 fertilizer inputs without affecting crop yields by improving plant nitrogen use efficiency
102 (NUE). This objective is challenging since NUE is a complex trait that includes uptake,
103 utilization and remobilization efficiencies of the whole plant or of specific organs such
104 as grains (Liu *et al.*, 2022). Therefore, research on NUE improvement has been tackled
105 through approaches engineering known molecular players (transporters, enzymes) or
106 heuristically by Quantitative Trait Loci (QTL), Genome-Wide Association Study
107 (GWAS) and transcriptome candidate genes approaches. However, to date, crop
108 varieties with optimized NUE are still rare (Liu *et al.*, 2022; Melino *et al.*, 2022;
109 Govindasamy *et al.*, 2023).

110 The large number of nitrate transport mechanisms and their multiple level of regulation
111 form a complex network coordinating nitrate fate and homeostasis. The latter is
112 illustrated by remarkably stable cytosolic nitrate levels ranging between 3 and 5 mM
113 (Cookson *et al.*, 2005). Once absorbed into root cells, nitrate has three possible fates
114 (Dechorgnat *et al.*, 2011). A first one is a direct export to vascular tissue partially
115 through xylem associated nitrate transporters. A second one is its assimilation where
116 cytosolic nitrate is reduced first by the nitrate reductase to nitrite and then by the
117 plastidial nitrite reductase to form ammonium. Ammonium is then incorporated into
118 organic acids to produce amino acids. The third fate of cytosolic nitrate is vacuolar
119 storage. The vacuolar compartment plays important roles in controlling of the plant

120 nitrate status as vacuolar nitrate accumulation has two major functions (Han *et al.*,
121 2016; Hodin *et al.*, 2023). First, vacuolar nitrate represents a temporary reserve of N
122 allowing a near constant cytoplasmic provision independently of external fluctuations
123 as nitrate concentrations in this compartment can reach up to 80 mM (van der Leij *et*
124 *al.*, 1998; Cookson *et al.*, 2005). Second, vacuolar nitrate acts as an osmoticum
125 contributing to the osmotic potential, including during stomata movements (McIntyre,
126 1997; Wege *et al.*, 2014; Hodin *et al.*, 2023).
127 The first nitrate/proton exchanger mediating nitrate influx into the vacuole, CLCa, was
128 characterized in Arabidopsis (De Angeli *et al.*, 2006). This protein is part of a family of
129 seven members in this species. CLCa and CLCb were shown to preferentially
130 exchange nitrate over chloride against proton (De Angeli *et al.*, 2006; Bergsdorf *et al.*,
131 2009; von der Fecht-Bartenbach *et al.*, 2010; Wege *et al.*, 2010; Barbier-Brygoo *et al.*,
132 2011). Both of these exchangers are located on the vacuolar membrane. CLCa activity
133 accounts for up to 50% of vacuolar nitrate content but can also be involved in nitrate
134 efflux from the vacuole in stomata depending of its state of phosphorylation (Geelen *et*
135 *al.*, 2000; Wege *et al.*, 2014). Impaired nitrate flux into vacuoles through CLCa was
136 shown to reduce nitrate uptake, nitrate content and expression level of several nitrate
137 transporter genes but to increase nitrate assimilation and consequently NUE
138 (Monachello *et al.*, 2009; Hodin *et al.*, 2023). As for CLCb, its participation in nitrate
139 accumulation could not been demonstrated as nitrate contents are at the same level
140 in wild type and *clcb* KO mutant when plants are grown in sufficient nitrate-condition
141 (von der Fecht-Bartenbach *et al.*, 2010). However, it was proposed recently that CLCb
142 mediates nitrate efflux from the vacuoles when plants are grown on low nitrate
143 concentrations (Shi *et al.*, 2023).
144 Next to CLC transporters, some members of NRT2 and NPF transporters family are
145 localized in the vacuolar membrane (Hu *et al.*, 2016; He *et al.*, 2017; Wang *et al.*, 2018;
146 Lu *et al.*, 2022). Among them, NRT2.7 belongs to the seven members of the *NRT2*
147 gene family in Arabidopsis that encode major high affinity nitrate transporters. All NRT2
148 proteins except NRT2.7 are localized at the plasma membrane. NRT2.7 forms indeed
149 a distinct monophyletic group within the Arabidopsis NRT2 family. The expression of
150 the *NRT2.7* gene occurs mainly in seeds, but its expression has been also described
151 for leaves and roots (Orsel *et al.*, 2002; Okamoto *et al.*, 2003; Chopin *et al.*, 2007).
152 NRT2.7 is able to mediate nitrate fluxes in Xenopus oocytes. The main phenotype of
153 *nrt2.7* knock-out mutants is a greatly decreased nitrate content in seeds which

154 highlights the major roles of NRT2.7 in nitrate accumulation at reproductive stage
155 (Chopin *et al.*, 2007).

156 Regarding nitrate as a signal, a nutrient or an electro-osmotic charge, further work in
157 characterizing transporters and channels involved in vacuolar fluxes will shed light on
158 the putative sensing and signaling properties of the largest compartment of plant cells.
159 The mechanism of nitrate transport by NRT2.7 was not investigated *in planta* as this
160 protein is essentially present in seeds. So, in this report, we first investigated the impact
161 of a NRT2.7 overexpression in Arabidopsis on nitrate homeostasis, activities of plasma
162 membrane nitrate uptake systems, growth and vacuolar nitrate currents. Functional
163 characterization of nitrate transporters *in planta* often requires the genetic removal of
164 the quantitatively most important components to uncover more subtle or fine-tuning
165 mechanisms. For example, the nitrate transport activity of NRT2 family members are
166 masked by the NRT2.1 activity and has to be assessed in the *nrt2.1* deficient
167 background (Chopin *et al.*, 2007; Kiba *et al.*, 2012; Lezhneva *et al.*, 2014). Here we
168 applied a similar strategy and used the *clca* mutant background in addition to a wild-
169 type background, to test the physiological impact of NTR2.7 activities *in planta* and to
170 determine by electrophysiology the effect the overexpression of NRT2.7 in *clca* on
171 vacuolar nitrate currents. We thus elucidate the function of NRT2.7 by asking the
172 following questions: (i) whether or not overexpression of NRT2.7 nitrate transporter
173 would give similar effects as overexpression of the CLCa nitrate exchanger in the *clca*
174 knock-out genetic background, (ii) how the *NRT2.7* overexpression in wild-type
175 background would affect nitrate homeostasis and growth under nitrate sufficient and
176 limiting conditions and, (iii) what are the consequences of *NRT2.7* overexpression on
177 nitrate fluxes through the vacuolar membrane.

178

179 **Material and methods**

180 Plant material and growth conditions

181 All *Arabidopsis thaliana* genotypes used in this study were obtained or generated in
182 the Wassilewskija (WS) background. The *clca-2* T-DNA knock-out plant line originates
183 from the Versailles collection (FST 171A06, line EAE89] whereas *clca-1* was isolated
184 in Geelen *et al.* (2000). The *CLCa-OX* (*clca-2*) line (*clca-2* knock-out mutant

185 overexpressing *CLCa* under the 35S promoter of the Cauliflower Mosaic Virus, CaMV)
186 originates from Wege *et al.* (2010). The *NRT2.7-OX* (*clca*) lines (*clca* knock-out mutant
187 overexpressing *NRT2.7* under the 35S promoter of the CaMV) was obtained by
188 crossing *NRT2.7* overexpressors (in the WS background, Chopin *et al.*, 2007) with the
189 *clca* mutants (*clca-1* and *clca-2*). The vectors used to over-express *CLCa* and *NRT2.7*
190 contain the three regions necessary for the activity of the *35S* promoter (Ow *et al.*,
191 1987).
192 Seeds were surface-sterilized, stored for 3 days at 4°C to synchronize germination and
193 sown in 120 x 120 mm square Petri dishes containing either 35 or 70 mL nutrient
194 medium to monitor root architecture (4-5 plants/plate) or to produce material for
195 analysis (12-15 plants/plate). Media differed in their nitrate content (0.2|2|20 mM) and
196 consisted respectively of 0.2|0.7|7 mM KNO_3; 0|0.65|6.5 mM $Ca(NO_3)_2$; 0.5|0.5|1.5 mM
197 $MgSO_4$; 0.625|0.625|0 mM KH_2PO_4; 0|0|1.875 mM NaH_2PO_4; 0.75|1.25|1.25 mM NaCl;
198 0.65|0.25|0 mM $CaCl_2$ and 1.05|0.55|0 mM KCl. For all media, micronutrients (in µM)
199 consisted of 42.5 FeNaEDTA, 0.16 $CuSO_4$, 45 H_3BO_3, 0.015 $(NH_4)_6Mo_7O_{24}$, 0.01
200 $CoCl_2$, 0.38 $ZnSO_4$, 1.8 $MnSO_4$. All media were supplemented with 1% sucrose, pH
201 balanced at 5.8 before autoclaving and solidified using 1% agar (Sigma A1296). Petri
202 dishes were sealed using 3M adhesive tape and placed below tubes delivering 65 µE
203 irradiance for 16h/day in a tissue culture room with a thermoperiod day/night of
204 22/18°C. At 12 days after germination (14 days after sowing), plants were harvested
205 (or sampled for ^{15}N uptake) between 10 and 12 am (after 3 to 5h light exposure).

206 Growth measurements

207 Root architecture was measured at 3, 6 and 9 days after germination by scanning Petri
208 dishes using a flat-bed scanner (Epson Perfection 4490 Photo) at a 200 dots per inch
209 resolution. Total root length was acquired by analyzing root morphology with the EZ-
210 Rhizo software (Armengaud *et al.*, 2009). Plant biomass was measured directly on a
211 microbalance (Mettler Toledo XS3DU) for fresh weight.

212 RNA extraction and RT-qPCR analysis

213 RNA was extracted from shoots using the Trizol reagent (Invitrogen) according to the
214 provider recommendations. One microgram was treated with DNase and reverse
215 transcribed using the Quantitect kit (Qiagen) following the manufacturer instructions.
216 For qPCR analysis, specific primers were used for *NRT2.7* (5'-

217 CCTTCATCCTCGTCCGTTTC-3' (forward) and 5'- AATTCGGCTATGGTGGAGTA-3'
218 (reverse)) and *EF1α* ((At5g60390) 5'- CTGGAGGTTTTGAGGCTGGTAT-3' (forward)
219 and 5'- CCAAGGGTGAAAGCAAGAAGA-3' (reverse)). The reactions were performed
220 in a Realplex mastercycler (Eppendorf) using commercial SYBR green mastermix
221 (Roche). Samples were subjected to 2 min pre-incubation at 95°C followed by 40
222 amplification cycles of 15 s at 95°C, 15 s at the melting temperature of the primers set
223 and 20 s at 68°C. *NRT2.7* transcript levels were quantified using linear regression of
224 quantified amplicon range and expressed relatively to *EF1α*.

225 Analysis of nitrate, total carbon, and total N contents

226 Frozen plant material was ground in liquid nitrogen using a Retsch mill grinder (MM301,
227 Retsch GmbH, Germany). For nitrate content determination, an aliquot of 20 mg of
228 frozen powder was used to prepare an ethanol-water extract as described in Cross *et*
229 *al.* (2006). Nitrate content was assayed after its reduction by vanadium(III) combined
230 with detection by the acidic Griess reaction as described in Miranda *et al.* (2001). Total
231 carbon (C) and N content were determined using an elemental analyzer (EA, Flash
232 2000, Thermo Scientific) on aliquots of 0.5 to 2 mg dry weight in tin capsules. EA
233 settings consisted of 20 sec of oxygen flux at 80 mL/min and helium at 140 mL/min for
234 5 min.

235 ^{15}N nitrate uptake measurements

236 Influx of $^{15}NO_3^-$ was assayed as previously described (Orsel *et al.*, 2004). Two to three
237 12-day-old plants were first transferred to 0.1 mM $CaSO_4$ for 1 min. To measure high
238 affinity ^{15}N nitrate uptake, plants were then transferred to a liquid 0.2 mM nitrate
239 containing medium (the same as described earlier but without sucrose) enriched at
240 99% with $^{15}NO_3^-$ (Sigma). To measure low affinity transport capacity, plants were
241 instead transferred to a 6 mM nitrate medium consisting of 3 mM $K^{15}NO_3$; 1.5 mM
242 $Ca(^{15}NO_3)_2$; 0.5 mM $MgSO_4$; 0.625 mM KH_2PO_4; 1.5 mM NaCl and the same
243 micronutrients as described before. ^{15}N nitrate uptake was performed for 5 min and
244 plants were finally incubated for 1 min in 0.1 mM $CaSO_4$. Roots were then placed into
245 tin capsules, dried at least 48h at 80°C and sent for ^{15}N elemental analysis using an
246 ANCA–MS system (PDZ Europa, Crewe, UK) at INRAE Montpellier. Nitrate uptake
247 was calculated from the ^{15}N content of the roots (0.5 to 1.5 mg DW). Each uptake
248 experiment included at least 5 measurements per condition and genotype.

249 Patch-clamp analyses

250 Patch-clamp experiments were made in the whole-vacuole configuration with an
251 access resistance between 1.5-3 MΩ. Patch-clamp recordings were made with an
252 EPC8 amplifier (HEKA, Lambrecht-Pfalz Germany). Data were acquired with an
253 AD/DA converter Instrutech LIH 8+8 under the control of the software PatchMaster
254 (HEKA, Lambrecht-Pfalz Germany) and analysed with FitMaster software (HEKA,
255 Lambrecht-Pfalz Germany). Applied membrane potentials were always corrected by
256 the liquid junction potential (Neher, 1992). Current to voltage characteristics were
257 obtained measuring the amplitude of the stationary current. Measurements were done
258 after waiting that the vacuolar lumen solution was equilibrated with the pipette solution,
259 typically 10 minutes after the establishment of the whole-vacuole configuration.
260 Cytosolic side solutions were changed using a gravity driven perfusion system. Bis-
261 Tris-propane (BTP) was chosen as a large impermeable cation in order to minimize
262 cation currents. The solution used for patch-clamp experiments were (in mM): Nitrate
263 vacuolar solution: 100 BTP, 200 HNO_3, 0.1 $CaCl_2$, 5 $MgCl_2$, 5 MES, pH = 5.5. Chloride
264 vacuole solution : 475 MES, 15 HCl, 60.5 BTP, 0.1 $CaCl_2$, pH = 5.5. Chloride cytosolic
265 solutions: 7.5 BTP, 15 HCl, 0.1 $CaCl_2$, 2 $MgCl_2$, 15 MES, pH = 7. Nitrate cytosolic
266 solution: 0.1 $Ca(NO_3)_2$, 2 $Mg(NO_3)_2$, 15 MES, pH = 7 with BTP. Osmotic pressures of
267 the cytosolic and vacuolar solutions were adjusted with sorbitol to 640 and 650 mOsm,
268 respectively.

269 Statistical analysis

270 Statistical analyses were conducted using the pairwisePermutationTest function from
271 the rcompanion package in the R environment, except for the electrophysiology
272 results. For those, a Mann-Whitney test was applied using GraphPad Prism 8 software.
273 All the raw data and the results of the statistical analysis can be found in the
274 supplementary table.
275

276 Results

277 Both *CLCa* and *NRT2.7* overexpression restore growth of the *clca-2* mutant

278 To set a suitable genetic background for NRT2.7 functional studies, we characterized
279 the phenotypes of *clca* mutants on a range of nitrate supplied as a sole nitrogen source

280 in vertical Petri dishes. We used *clca-1* and *clca-2* knock-outs (Geelen *et al.*, 2000;
281 De Angeli *et al.*, 2006) which both showed a significant decrease in shoot fresh weight
282 (-13 to -45%) and root growth rate (-8 to -40%) when compared to the WS wild type
283 (Fig. 1, Supplementary Fig. S1A, B and S2A, B). This decrease was more pronounced
284 under non-limiting nitrate supply (2 and 20 mM). As expected, *clca mutants* showed
285 reduced nitrate content compared to WS under all N supplies in both shoot and root
286 (Supplemental Fig. S1C, D and S2C, D).
287 To study the activity of NRT2.7, we overexpressed ectopically *NRT2.7* in the *clca-2*
288 background and as control in WS. To produce the different genotypes, we used the
289 *NRT2.7*-overexpressing lines *NRT2.7-Ox1 (*WS*)* and *NRT2.7-Ox2 (*WS*)* generated in
290 a previous study (Chopin *et al.*, 2007) and analysed the *NRT2.7* expression in aerial
291 part. It was very weakly expressed in WS whereas the level of its mRNA is very high
292 in *NRT2.7-Ox1 (*WS*)* and *NRT2.7-Ox2 (*WS*)* (Supplementary Fig. S3). These two lines
293 were crossed with the *clca* mutant to obtain *NRT2.7-Ox1* (*clca-2*) and *NRT2.7-Ox2*
294 (*clca-2*), expressing consequently *NRT2.7* at the same level than in the WS
295 background. *NRT2.7-Ox1* (*clca-2*) and *NRT2.7-Ox2* (*clca-2*) showed similar
296 phenotypes and representative data for one line are presented. For comparison, we
297 included in our studies a *clca-2* mutant overexpressing the *CLCa* cDNA under the
298 control of the strong 35S promoter of the CaMV (referred thereafter as *CLCa-Ox* (*clca-*
299 *2)*) (Wege *et al.*, 2010). In this line, *CLCa* transcript levels were increased 30-fold
300 compared to WS (Wege *et al.*, 2014).
301 Based on the more pronounced differences in growth between *clca-2* and WS under
302 non-limiting external N supply, we cultivated the plants on 2 mM nitrate medium for all
303 further analyses using both *clca-2* lines overexpressing either *CLCa* or *NRT2.7*
304 compared to the controls WS, *NRT2.7* over-expressing lines (*NRT2.7-Ox1* (WS)) and
305 *clca-2.* Both *CLCa* and *NRT2.7* overexpression restored the *clca-2* growth phenotypes
306 for shoot biomass and total root length (Fig. 1). This growth restoration was also
307 observed in both lines overexpressing *NRT2.7* in the *clca-1* knock-out background and
308 occurred regardless external nitrate availability (Supplementary Fig. S2A, B). Wild-type
309 plants overexpressing *NRT2.7* showed an important increase of 60% in total root
310 length and no significant difference in shoot fresh weight compared to WT (Fig. 1B,
311 C). The growth stimulation observed for *NRT2.7* overexpressing lines both in the *clca-*
312 *2* and the WS background, is therefore independent of the *clca-2* mutation. The

313 physiological changes triggered by *NRT2.7* overexpression in the *clca* mutants are
314 thus different from the complementation by *CLCa* while both led to restored growth.

315 *NRT2.7* and *CLCa* overexpression have opposite effects on both nitrate content and
316 nitrate uptake capacities

317 To decipher the underlying mechanism that impact growth of these overexpressing
318 lines, we determined nitrate content in roots and shoots. As described earlier (Wege
319 *et al.*, 2010), nitrate content of *clca-2* was 35 and 28 % lower than WT level in shoots
320 and roots, respectively (Fig. 2A, C). Expression of *CLCa* in the *clca-2* mutant restored
321 nitrate levels in shoots and roots, whereas *NRT2.7* overexpression in the *clca-2*
322 background led to a 53% decrease of the nitrate content when compared with the *clca-*
323 *2* mutant (Fig. 2A, C). Likewise, *NRT2.7* overexpression does not complement *clca-1*
324 phenotype for shoot and root nitrate content regardless the external nitrate
325 concentration for plant growth (Supplementary Fig. S2C, D). This showed that the
326 increased growth observed in the *NRT2.7-Ox (clca-2)* and *NRT2.7-Ox (clca-1)* lines
327 occurred without restoring nitrate content. Like the effect of *NRT2.7* overexpression in
328 the *clca-2* mutant background, overexpression of *NRT2.7* in wild-type background was
329 accompanied by a slight decrease in nitrate content in roots but no significant
330 modification was observed in shoots (Fig. 2B, D).

331 In order to understand the impact on nitrate levels, we investigated how nitrate uptake
332 was affected in these lines. Nitrate uptake was measured using ^{15}N labelled nitrate at
333 concentration of 0.2 and 6 mM to monitor both high and low affinity transport system
334 activities (HATS and LATS, respectively, this latter activity being obtained as the
335 difference between uptake measurements at 6 mM and 0.2 mM). Figure 3 shows that
336 the HATS activity was decreased by 16% in *clca-2* whereas the LATS activity was not
337 significantly different from that of WT. The *CLCa-Ox* (*clca-2*) line exhibited the same
338 uptake capabilities for both transport activities as wild-type plants, illustrating a full
339 complementation of the *clca-2* mutant phenotype. The *NRT2.7-Ox* (*clca-2*) line showed
340 similar HATS activity as the *clca-2* knock-out mutant but an increase by 29% of LATS
341 activity (Fig. 3B, C). The *NRT2.7-Ox* (WS) lines displayed comparable profiles but
342 enhanced effect with a 2-fold increased activity of the LATS when compared to WT
343 (Fig. 3C). Thus, whereas *CLCa* overexpression in the *clca* mutants increased mainly
344 HATS activity compared to WT, *NRT2.7* overexpression had the opposite effect,

345 supporting the hypothesis that these two nitrate transporters have different functions
346 *in planta* when overexpressed ectopically.

347 *NRT2.7* overexpression leads to increased biomass under limiting and non-limiting
348 conditions

349 Plants stimulate their root growth when their N nutritional status is low (Jia and von
350 Wirén, 2020). Given the important increase of root growth in the *NRT2.7-Ox* (WS) lines
351 under non-limiting N supply (Fig. 1), we further studied the growth-promoting effect of
352 *NRT2.7* overexpression under limiting N supply to better understand the impacts of the
353 changes in nitrate fluxes through the vacuolar membrane. Plants were grown on
354 vertical agar medium containing 0.2 mM nitrate for 12 days. In these conditions, shoot
355 biomass and total root length of *NRT2.7-Ox* (WS) lines were increased when compared
356 to WT by 49 to 65% and 19 to 33% respectively (Fig. 4A, B). Conversely, root nitrate
357 content of the *NRT2.7-Ox* (WS) lines was dramatically reduced by 75 to 83% compared
358 to WT, whereas shoot nitrate content was not modified (Fig. 4C, D). A similar tendency
359 was observed when *NRT2.7* was overexpressed in *clca* KO mutant comparing nitrate
360 content to shoot and root biomass (Supplementary Fig. S4).
361 The carbon to nitrogen (C/N) ratio is an essential indicator that plants perceive to
362 orientate their growth, development and metabolism (Coruzzi and Zhou, 2001). The
363 C/N ratio of *NRT2.7-Ox* (WS) compared to WT was increased in shoots and roots
364 mainly due to a decrease in total N proportion (Fig. 4E). These data suggest that the
365 ectopic expression of *NRT2.7* drives nitrate use for biomass production. As no
366 difference in nitrate uptake through the HATS was observed (Fig. 3), the strong
367 decrease in nitrate content could be the consequence of a lower vacuolar storage
368 capacity and/or an increased nitrate flux out of the vacuole as it was previously shown
369 for other vacuolar nitrate transporters (He *et al.*, 2017; Lu *et al.*, 2022; Hodin *et al.*,
370 2023; Shi *et al.*, 2023).

371 *NRT2.7* overexpression leads to increased nitrate fluxes out of the vacuole

372 In order to associate the observed physiological changes with NRT2.7 functional
373 properties, we used an electrophysiological approach to determine if the over-
374 expression of *NRT2.7* modifies the nitrate fluxes across the vacuolar membrane. We
375 took advantage of the *NRT2.7-Ox* (*clca-2*) line where such modification would not be
376 masked by CLCa-driven fluxes. We extracted vacuoles from mesophyll protoplasts of

377 the *clca-2* and the two *NRT2.7-Ox* lines (*clca-2*) and performed patch clamp
378 experiments in whole-vacuole configuration (Fig. 5). In order to maximize the fluxes of
379 nitrate directed from the vacuole to the cytosol and from the cytosol to the vacuole, we
380 performed two independent series of experimentations designed as follow. In both
381 experiment series, we used the non-permeant cation BisTriPropane in order to limit
382 the vacuolar currents mediated by cations. With the aim to highlight the efflux of nitrate
383 from the vacuole (positive ionic currents), in the first series of experiments (Fig. 5B),
384 we used bi-ionic conditions with 200 mM nitrate in the vacuole and 19.2 mM chloride
385 in the cytosolic-side solution. The vacuoles extracted from *clca-2* knock-outs presented
386 a mean current density of +1.3 ± 0.4 pA/pF at +43 mV and a mean reversal potential
387 (E_{rev}=-8 ± 3 mV) that were comparable to those previously observed in similar ionic
388 conditions (De Angeli *et al.*, 2006; Wege *et al.*, 2010). Importantly, in the same ionic
389 conditions, vacuoles from *NRT2.7-Ox (clca-2)* plants presented significantly higher
390 current densities compared to *clca-2* currents only at positive vacuolar membrane
391 potentials (from +3 mV to +83 mV, Fig. 5B). To note, similar results were obtained for
392 both lines as displayed on the figures by vertical or horizontal diamonds. These positive
393 currents are compatible with an increased nitrate efflux capacity of the vacuoles from
394 *NRT2.7-Ox (clca-2)* plants. In the second set of experiments, we used an ionic
395 configuration suited to highlight nitrate currents directed from the cytosol to the
396 vacuolar lumen. We performed cytosolic-side solution exchange experiments starting
397 from a chloride-based buffer (19.2 mM Cl^- pH 7) to a nitrate based buffer (4 mM NO_3^-
398 pH 7) keeping the vacuolar-side buffer constant and with only chloride as a permeant
399 anion (15 mM Cl^- pH 5.5) (Supplementary Fig. S5A and S5B). Upon the exchange of
400 the cytosolic-side solution a similar increase of the negative current was observed in
401 vacuoles obtained from the tested genotypes. Indeed, the mean current ratios at -60
402 mV were I_{NO3}/I_{Cl}=1.84±0.4 in *NRT2.7-Ox (clca-2)* vacuoles and I_{NO3}/I_{Cl}=1.77 ± 0.44 in
403 *clca-2* vacuole*s*. Conversely, the current densities in presence of nitrate did not show
404 a significant difference between the genotypes, being I_{NO3}=-2.4±1 pA/pF at -60 mV in
405 *NRT2.7-Ox* (*clca-2*) and I_{NO3}=-2.7±0.9 pA/pF at -60 mV in *clca-2.* As the current
406 amplitudes in *NRT2.7* overexpressor show a high variability compared to those of the
407 *clca-2* mutant, we checked whether the rectification ratios between the currents at +83
408 mV versus -77 mV and +63 mV versus -57 mV (Supplementary Fig. S5C and S5D)
409 were not different between the vacuoles from the different genotypes. The values of
410 these ratios were around -3 and there was no significant difference between the two

411 genotypes. Further no correlation between the rectification ratio (I_{+83mV}/I_{-77mV}) and
412 current density (I_{+83mV}) could be identified. This indicates that the high variability of
413 currents obtained in *NRT2.7*-Ox (*clca-2*) is not linked to background leak currents. In
414 conclusion, this second series of experiments indicates that the vacuoles obtained
415 from *NRT2.7-Ox* (*clca-2*) do not display an increased capacity of driving NO_3^- fluxes
416 directed to the vacuolar lumen compared to the vacuoles from *clca-2* under our
417 experimental conditions. Altogether, the results obtained by patch-clamp experiments
418 suggest that, compared to vacuoles from *clca-2*, *NRT2.7-Ox* (*clca-2*) plant vacuoles
419 present a higher capacity to drive nitrate fluxes directed into the cytosol but are not
420 modified concerning nitrate influx into the vacuole.

421

422 ## Discussion

423 Recent studies underline the importance of nitrate fluxes through the vacuolar
424 membrane to enhance NUE by increasing efflux of nitrate from vacuole and/or reducing
425 nitrate storage in this latter compartment (Han *et al.*, 2016; Wang *et al.*, 2018; Hodin
426 *et al.*, 2023; Shi *et al.*, 2023). It is therefore essential to characterize the different
427 vacuolar nitrate transporters and their activities to get a better understanding of their
428 functional specificities. In this report, we analyzed the function of the vacuolar NRT2.7
429 transporter by introducing its cDNA under the control of the *35S* promoter in *clca* KO
430 mutant or in wild type. The combined results of the electrophysiological analyses and
431 physiological traits of the *CLCa* and *NRT2.7* overexpressing lines strikingly
432 demonstrate that both NRT2.7 and CLCa impact N use but through clearly distinct
433 mechanisms. The *NRT2.7* overexpression in the *clca-2* mutant bypassed the CLCa-
434 dependent reduced growth via a mechanism that uncoupled growth and nitrate
435 accumulation probably related to modified nitrate efflux from the vacuole. This
436 mechanism, when acting in a wild-type background overexpressing *NRT2.7*, led to an
437 increase of biomass production mainly through a higher root biomass.

438 NRT2.7 stimulates nitrate export out of the vacuole when overexpressed ectopically

439 In this study, we used the *CLCa* mutant altered physiology to assess functions and
440 physiological consequences of *NRT2.7* ectopic expression. We chose CLCa over its
441 closest homologous, CLCb, as the *clca* KO mutant has a stronger phenotype than *clcb*

442 in respect to nitrate contents (Geelen *et al.*, 2000; von der Fecht-Bartenbach *et al.*,
443 2010; Shi *et al.*, 2023) and, nitrate currents are very small in *clca* even when *CLCb* is
444 over-expressed into this mutant compared to wild type (De Angeli *et al.*, 2006;
445 Monachello *et al.*, 2009). Furthermore, similar to CLCb, CLCa is involved in nitrate
446 efflux out the vacuole depending on its phosphorylation state (Wege *et al.*, 2014). As
447 the phosphorylation site is conserved in CLCb, we can assume that CLCb could work
448 in both ways depending on the growth conditions.
449 In this study, we confirmed that *CLCa* mutant physiology was deeply affected by its
450 limiting capacity of loading nitrate into vacuoles (Fig. 1 and 2; Supplementary Fig. S1
451 and S2). Besides CLCa, the NRT2.7 nitrate transporter is located at the tonoplast and
452 has been showed to translocate nitrate in Xenopus oocytes. Its loss-of-function
453 reduces nitrate accumulation in seeds where the gene is chiefly expressed (Chopin *et*
454 *al.*, 2007). Although *NRT2.7* mRNA were detected in leaves and roots, no phenotype
455 other than seed traits have been reported in the KO mutant (Orsel *et al.*, 2002;
456 Okamoto *et al.*, 2003; Chopin *et al.*, 2007).
457 To better characterize its function *in planta*, we overexpressed *NRT2.7* in wild type and
458 *clca* KO mutant backgrounds. The overexpression of *NRT2.7* fully restores the reduced
459 *clca-2* plant growth and even exceeds wild-type biomass but, surprisingly, further
460 diminished the low *clca-2* nitrate content (Fig. 1 and 2). It led to 35% and 23%
461 decreases of shoot and root nitrate pools, respectively, when compared to *clca-2*.
462 These results showed that *NRT2.7* could indeed rescue the *clca-2* growth defect but
463 rather through an alternative mechanism than a true functional complementation. This
464 hypothesis was confirmed as the *NRT2.7* overexpressors in both wild-type and *clca-2*
465 background showed an increase in total root length and a depletion of root nitrate
466 content compared to wild-type plants.
467 The decrease of root nitrate content caused by *NRT2.7* ectopic overexpression is
468 difficult to conceive with a vacuolar nitrate importer. Chopin *et al.* (2007) reported an
469 influx of ^{15}N labeled nitrate into NRT2.7 expressing oocytes. This result indicates that,
470 in this biological system, NRT2.7 was targeted to the plasma membrane with
471 presumably its cytoplasmic N- and C-terminal domains oriented to the oocyte
472 cytoplasm. *In planta*, NRT2.7 is localized at the tonoplast (Chopin *et al.*, 2007). As
473 NRT2.7 cytoplasmic terminus is probably maintained in the plant cell cytoplasm
474 (Jacquot *et al.*, 2020), NRT2.7 would thus function as a nitrate efflux system from the
475 vacuole to the cytoplasm. This orientation is in agreement with the fact that NRT2s are

476 H^+/NO_3^- symporters (Forde and Clarkson, 1999) and that roots of *NRT2.7*
477 overexpressors become depleted of nitrate at low external nitrate availability (Fig. 4,
478 Supplementary Fig. S4). In addition, the determination of nitrate fluxes by patch clamp
479 techniques showed that isolated vacuoles from *NRT2.7-Ox* (*clca-2*) plants displayed a
480 higher capacity to drive nitrate fluxes directed to the cytosol th an isolated vacuoles
481 from *clca-2* plants (Fig. 5). The difference of current density between the two genotypes
482 is rather small (i.e about 1.3 pA/pF more in *NRT2.7-Ox* (*clca-2*) vacuoles at +63 mV).
483 This can be explained by a difference of electrogenicity and unitary turnover rate
484 between the two kinds of ion transporters, CLCa being a nitrate/proton antiporter and
485 NRT2.7 a nitrate/proton symporter (Forde and Clarkson, 1999; De Angeli *et al.*, 2006).
486 In the same experimental setup, we showed that the capacity of such isolated vacuoles
487 to drive nitrate influx did not vary between these genotypes (Fig. 5 and Supplementary
488 Fig. S5). This indicates that NRT2.7 stimulates vacuolar nitrate export when ectopically
489 overexpressed in seedlings and could explain the observed decrease in nitrate content
490 when *NRT2.7* is overexpressed in *clca-2* background. As this latter effect was also
491 detected in *NRT2.7-Ox* (WS) mainly when the plants were grown on 0.2 mM nitrate
492 (Fig. 4 and Supplementary Fig. S4), the activity of NRT2.7 to stimulate nitrate export
493 does not seem to rely on the import activity of CLCa. Additionally, based on these
494 experiments, we cannot completely exclude that NRT2.7 may regulate positively the
495 activity of nitrate exporters localized in the tonoplast and is not itself the active
496 transporter driving the fluxes. *CLCb*, recently shown to be a nitrate exporter when
497 nitrate is low in the external medium and, overexpressed in *clca* KO mutant
498 (Monachello *et al.*, 2009; Shi *et al.*, 2023), could have its activity induced by *NRT2.7*
499 overexpression. However, the decrease of root nitrate content by -75 and -83% in
500 *NRT2.7-Ox* (WS) compared to wild type was accompanied by a total root growth
501 increase of 33% when plants are grown on 0.2 mM nitrate (Fig. 4). Under the same
502 growth conditions, a similar tendency was observed in *NRT2.7-Ox* (*clca2),* a 19%
503 increase in root length was accompanied by a 84% reduction in root nitrate content
504 (Supplementary Fig. S4). As *CLCb* is over-expressed in *clca* mutant (Monachello *et*
505 *al.*, 2009), this that CLCb might not be involved in the stimulation of nitrate export by
506 *NRT2.7* overexpression.
507 Chopin *et al.* (2007) observed a decrease in seed nitrate content in *nrt2.7* mutants,
508 which was interpreted as a reduced capacity to import nitrate into the vacuole of the
509 embryo. *NRT2.7* is highly expressed in seeds and the *NRT2.7* promoter drives

510 expression in the embryos where the protein is located at the tonoplast. A decreased
511 nitrate content is thus difficult to explain by the loss-of-function of a vacuolar nitrate
512 exporter protein. However, the transport direction of NRT2.7 in seeds and in shoot/root
513 vacuoles might be different because of distinct types of vacuoles existing in these
514 organs (Shimada *et al.*, 2018). In addition, tonoplast membrane potential might vary
515 and the transport direction may reflect the organ specific ionic and osmotic conditions
516 as it has been discussed previously for NPF6.3 (NRT1.1/CHL1, (Léran *et al.*, 2014) or
517 CLCa (Wege *et al.*, 2014). Besides, nitrate transport properties are regulated via
518 posttranslational protein modifications (e.g. Wege *et al.*, 2014; Jacquot *et al.*, 2017), a
519 mechanism that should be explored in the future for NRT2.7. However, no
520 phosphorylation site in NRT2.7 is found in the PhosPhAt databases (Heazlewood *et*
521 *al.*, 2008). Finally, another hypothesis would be that *nrt2.7* seed nitrate content is
522 decreased because nitrate transport from the roots or shoots towards the seeds is
523 diminished in the *nrt2.7* mutants. Indeed, in Arabidopsis seeds, nitrate content seems
524 to rely directly on the nitrate taken up by roots (Schulze *et al.*, 1994). Inflorescence
525 grafting experiments are required to distinguish between seed prone or root/shoot
526 prone determination of the decreased nitrate level in *nrt2.7* seeds. Altogether, these
527 results support that NRT2.7 is essential for nitrate fluxes through the vacuolar
528 membrane. It stimulates nitrate export from the vacuole in seedlings but the contrasting
529 phenotype in reproductive and vegetative organs when the expression of *NRT2.7* is
530 modified, poses a challenging hypothesis and needs further investigation.

531 Nitrate fluxes through CLCa and NRT2.7 alter root nitrate uptake

532 As previously reported, we confirmed that the mutation in *CLCa* reduced nitrate uptake
533 activity in the high affinity range (Monachello *et al.*, 2009, Fig. 3) whereas the level of
534 LATS activity was not modified. These results illustrate the existence of a coordinated
535 signaling crosstalk between vacuolar and plasma membrane nitrate fluxes. An obvious
536 signal for this coordinated transmembrane transport would be the nitrate anion itself. It
537 was shown that loss of function of CLCa leads to a faster increase of the cytosolic
538 nitrate concentration in response to an increase of the extracellular NO_3^- concentration
539 in guard cells (Demes *et al.*, 2020). In this scenario, a transitory elevated cytosolic
540 nitrate level would decrease nitrate uptake, increase the nitrate efflux from the cells
541 and/or the assimilation pathways through the nitrate reductase (NR). This was
542 confirmed in a recent study demonstrating that the inhibition of nitrate storage in the

543 vacuole leads to an increase of the NR activity and a better NUE (Hodin *et al.*, 2023).
544 In addition to nitrate, nutrient uptake activity is controlled by a wide range of biophysical
545 (membrane potential, pH) or physiological signals (phosphorylation, metabolites) (see
546 Amtmann and Blatt, 2009). CLCa through its activity as a NO_3^-/H^+ exchanger is known
547 for its function in adjusting the cytosolic pH in guard cells (Demes *et al.*, 2020). More
548 recently, Jain and Schmidt (2024) showed that NRT2.1 phosphorylation level varies
549 according to the environmental pH certainly to adjust cytosolic pH. Then the loss of
550 function of *CLCa* could lead to the inactivation of NRT2.1 to compensate the change
551 in cytosolic pH.
552 The increase of nitrate export from the vacuole due to the *NRT2.7* overexpression
553 leads probably to change in nitrate cytosolic content and/or cytosolic pH, as for *clca-2*.
554 Even if this hypothesis needs to be tested using the nitrate/pH biosensor, ClopHensor
555 (Demes *et al.*, 2020), these modifications could explain the decrease in HATS activity
556 observed in *NRT2.7-Ox (clca-2)* like in *clca-2* plants but not the increase of the LATS
557 activity (Fig. 3). This latter discrepancy could suggest that alterations in nitrate influx
558 and efflux in and out of the vacuole do not have the same effect on nitrate uptake. The
559 coordination between the direction of vacuolar nitrate fluxes and nitrate influx at the
560 plasma membrane will need to be further studied in the future.

561 *NRT2.7* overexpression increases growth at low external and internal nitrate

562 The overexpression of *NRT2.7* stimulates nitrate export from the vacuole, leading to
563 an increase in plant growth. This phenotype could be explained not only by the
564 increase of LATS activity but also by a higher nitrate long-distance transport from root
565 to shoot. A study characterizing two *Brassica napus* genotypes differing by their
566 capacity in nitrate storage in root previously showed that the decrease of root nitrate
567 content induces a higher nitrate translocation from root to shoot leading to a better
568 NUE (Han *et al.*, 2016). We can assume that a similar phenomenon occurred in the
569 *NRT2.7* overexpressors.

570 Interestingly, both shoot and root biomass increased in *NRT2.7-Ox* (WS) grown under
571 limiting N nutrition even that a severe decrease of nitrate in root (-75 to -83% compared
572 to wild type) and a slight decrease of total nitrogen content (-8 to –19% compared to
573 wild type) occurred in these growth conditions (Fig. 4). These results confirm an
574 apparent disconnection between growth and nitrate content in *NRT2.7* overexpressors

575 plants. C and N metabolism are interconnected and regulate each other (Zheng, 2009).
576 Interestingly, the C/N ratio was higher in the overexpressors compared to wild type due
577 to a decrease in N proportion indicating that, even if plants are grown under low
578 external N availability, the overexpressors are able to maintain C proportions by
579 regulating photosynthesis activity facilitating the increase in biomass. The low internal
580 nitrate levels could be then the consequence of N dilution occurring under accelerated
581 growth. At the opposite, the increase of nitrate export from the vacuole could stimulate
582 nitrate assimilation and consequently photosynthesis as shown in a *Brassica napus*
583 genotype with reduced root nitrate storage (Han *et al.*, 2016) or, more recently when
584 Arabidopsis plants overexpressing the CLCb nitrate vacuolar exporter are grown on
585 low nitrate (Shi *et al.*, 2023).

586 In conclusion, we show that the two vacuolar nitrate transporters CLCa and NRT2.7
587 share limiting functionality and are not exchangeable. Our results suggest that NRT2.7
588 stimulates vacuolar nitrate export when overexpressed ectopically. By exploiting
589 genotypes with modified levels of vacuolar transporters, we show that changes in the
590 nitrate influx or efflux from the vacuolar compartment lead to differences in root nitrate
591 uptake suggesting the existence of a fine regulation between vacuolar and plasma
592 membranes through biophysical and physiological networks of vacuolar nitrate sensing
593 and homeostasis. NRT2.7, whose function *in vivo* seemed to be restricted to seeds,
594 triggers new physiological features when ectopically overexpressed. The link between
595 NRT2.7-driven nitrate fluxes and C content requires further studies but may be the
596 basis for improving plants with higher C/N ratios accompanied by increased growth
597 when N is limiting.

598

599 **Supplementary data**

600 The following supplementary data are available at *JXB* online.

601 Fig. S1. Growth and nitrate content of *clca-2* knock-out mutant grown on different
602 nitrate concentrations.

603 Fig. S2. Growth and nitrate content of *NRT2.7* overexpressors in the c*lca-1* knock-out
604 mutant.

605 Fig. S3. Level of NRT2.7 expression in *NRT2.7-Ox* (WS) lines.

606 Fig. S4. Effect of limiting N supply on the phenotype of *NRT2.7* over-expressors in
607 *clca-2* background.
608 Fig. S5. Nitrate influx in vacuoles from *NRT2.7*-Ox (*clca-2*) plants and from *clca-2*
609 knock-out.

610 **Acknowledgements**
611 The authors are very grateful to Pascal Tillard for servicing the ^{15}N measurements,
612 Anne Marmagne for helping with the elementary C/N analyzer and the IJPB platform
613 'The Plant Observatory', in particular Joël Talbotec and Philippe Maréchal for taking
614 care of greenhouse cultures.

615 **Author contributions**
616 FDV, AK and SF : conceptualization design ; PA, FDV, ADA, AK and SF: experimental
617 design ; PA, ADA, PB and VB performed the experimental work ; PA, MD, FDV, ADA,
618 AK and SF analyzed the data; PA, FDV, AK and SF wrote the manuscript. All authors
619 reviewed the manuscript.

620 **Conflict of interest**
621 The authors declare no conflict of interest.

622 **Funding**
623 This work benefits from the support of the LabEx Saclay Plant Sciences-SPS (ANR-
624 10-LABX-0040-SPS) and of the Agence Nationale de la Recherche (ANR-Nitrapool
625 ANR08-Blan-008).

626 **Data availability**
627 All the raw data supporting the findings of this work are available upon request from
628 the corresponding authors, Anne Krapp and Sophie Filleur. Statistical analyses are
629 available in the supplementary table 1.

630

631 ## References

632 **Amtmann A, Blatt MR**. 2009. Regulation of macronutrient transport. The New Phytologist
633 **181**, 35–52.

634 **Armengaud P, Zambaux K, Hills A, Sulpice R, Pattison RJ, Blatt MR, Amtmann A**. 2009. EZ-
635 Rhizo: integrated software for the fast and accurate measurement of root system
636 architecture. The Plant Journal: For Cell and Molecular Biology **57**, 945–956.

637 **Barbier-Brygoo H, De Angeli A, Filleur S, Frachisse J-M, Gambale F, Thomine S, Wege S**. 2011.
638 Anion channels/transporters in plants: from molecular bases to regulatory networks. Annual
639 Review of Plant Biology **62**, 25–51.

640 **Bergsdorf E-Y, Zdebik AA, Jentsch TJ**. 2009. Residues important for nitrate/proton coupling in
641 plant and mammalian CLC transporters. The Journal of Biological Chemistry **284**, 11184–
642 11193.

643 **Cassman KG, Dobermann A, Walters DT**. 2002. Agroecosystems, nitrogen-use efficiency, and
644 nitrogen management. Ambio **31**, 132–140.

645 **Chopin F, Orsel M, Dorbe M-F, Chardon F, Truong H-N, Miller AJ, Krapp A, Daniel-Vedele F**.
646 2007. The Arabidopsis ATNRT2.7 nitrate transporter controls nitrate content in seeds. The
647 Plant Cell **19**, 1590–1602.

648 **Cookson SJ, Williams LE, Miller AJ**. 2005. Light-dark changes in cytosolic nitrate pools depend
649 on nitrate reductase activity in Arabidopsis leaf cells. Plant Physiology **138**, 1097–1105.

650 **Coruzzi GM, Zhou L**. 2001. Carbon and nitrogen sensing and signaling in plants: emerging
651 'matrix effects'. Current Opinion in Plant Biology **4**, 247–253.

652 **Cross JM, von Korff M, Altmann T, Bartzetko L, Sulpice R, Gibon Y, Palacios N, Stitt M**. 2006.
653 Variation of enzyme activities and metabolite levels in 24 Arabidopsis accessions growing in
654 carbon-limited conditions. Plant Physiology **142**, 1574–1588.

655 **De Angeli A, Monachello D, Ephritikhine G, Frachisse JM, Thomine S, Gambale F, Barbier-**
656 **Brygoo H**. 2006. The nitrate/proton antiporter AtCLCa mediates nitrate accumulation in plant
657 vacuoles. Nature **442**, 939–942.

658 **Dechorgnat J, Nguyen CT, Armengaud P, Jossier M, Diatloff E, Filleur S, Daniel-Vedele F**.
659 2011. From the soil to the seeds: the long journey of nitrate in plants. Journal of Experimental
660 Botany **62**, 1349–1359.

661 **Demes E, Besse L, Cubero-Font P, Satiat-Jeunemaitre B, Thomine S, De Angeli A**. 2020.
662 Dynamic measurement of cytosolic pH and [NO3 -] uncovers the role of the vacuolar
663 transporter AtCLCa in cytosolic pH homeostasis. Proceedings of the National Academy of
664 Sciences of the United States of America **117**, 15343–15353.

von der Fecht-Bartenbach J, Bogner M, Dynowski M, Ludewig U. 2010. CLC-b-mediated NO-3/H+ exchange across the tonoplast of Arabidopsis vacuoles. Plant & Cell Physiology **51**, 960–968.

Forde BG, Clarkson DT. 1999. Nitrate and Ammonium Nutrition of Plants: Physiological and Molecular Perspectives. In: Callow JA, ed. Advances in Botanical Research. Academic Press, 1–90.

Geelen D, Lurin C, Bouchez D, Frachisse JM, Lelièvre F, Courtial B, Barbier-Brygoo H, Maurel C. 2000. Disruption of putative anion channel gene AtCLC-a in Arabidopsis suggests a role in the regulation of nitrate content. The Plant Journal: For Cell and Molecular Biology **21**, 259–267.

Govindasamy P, Muthusamy SK, Bagavathiannan M, *et al.* 2023. Nitrogen use efficiency-a key to enhance crop productivity under a changing climate. Frontiers in Plant Science **14**, 1121073.

Han Y-L, Song H-X, Liao Q, *et al.* 2016. Nitrogen Use Efficiency Is Mediated by Vacuolar Nitrate Sequestration Capacity in Roots of Brassica napus. Plant Physiology **170**, 1684–1698.

He Y-N, Peng J-S, Cai Y, Liu D-F, Guan Y, Yi H-Y, Gong J-M. 2017. Tonoplast-localized nitrate uptake transporters involved in vacuolar nitrate efflux and reallocation in Arabidopsis. Scientific Reports **7**, 6417.

Heazlewood JL, Durek P, Hummel J, Selbig J, Weckwerth W, Walther D, Schulze WX. 2008. PhosPhAt: a database of phosphorylation sites in Arabidopsis thaliana and a plant-specific phosphorylation site predictor. Nucleic Acids Research **36**, D1015-1021.

Hodin J, Lind C, Marmagne A, *et al.* 2023. Proton exchange by the vacuolar nitrate transporter CLCa is required for plant growth and nitrogen use efficiency. The Plant Cell **35**, 318–335.

Howarth RW, Marino R. 2006. Nitrogen as the limiting nutrient for eutrophication in coastal marine ecosystems: Evolving views over three decades. Limnology and Oceanography **51**, 364–376.

Hu R, Qiu D, Chen Y, Miller AJ, Fan X, Pan X, Zhang M. 2016. Knock-Down of a Tonoplast Localized Low-Affinity Nitrate Transporter OsNPF7.2 Affects Rice Growth under High Nitrate Supply. Frontiers in Plant Science **7**, 1529.

Jacquot A, Chaput V, Mauries A, *et al.* 2020. NRT2.1 C-terminus phosphorylation prevents root high affinity nitrate uptake activity in Arabidopsis thaliana. The New Phytologist **228**, 1038–1054.

Jacquot A, Li Z, Gojon A, Schulze W, Lejay L. 2017. Post-translational regulation of nitrogen transporters in plants and microorganisms. Journal of Experimental Botany **68**, 2567–2580.

Jain D, Schmidt W. 2024. Protein Phosphorylation Orchestrates Acclimations of Arabidopsis Plants to Environmental pH. Molecular & cellular proteomics: MCP **23**, 100685.

Jia Z, von Wirén N. 2020. Signaling pathways underlying nitrogen-dependent changes in root system architecture: from model to crop species. Journal of Experimental Botany **71**, 4393–4404.

Kiba T, Feria-Bourrellier A-B, Lafouge F, *et al.* 2012. The Arabidopsis nitrate transporter NRT2.4 plays a double role in roots and shoots of nitrogen-starved plants. The Plant Cell **24**, 245–258.

van der Leij M, Smith SJ, Miller AJ. 1998. Remobilisation of vacuolar stored nitrate in barley root cells. Planta **205**, 64–72.

Léran S, Varala K, Boyer J-C, *et al.* 2014. A unified nomenclature of NITRATE TRANSPORTER 1/PEPTIDE TRANSPORTER family members in plants. Trends in Plant Science **19**, 5–9.

Lezhneva L, Kiba T, Feria-Bourrellier A-B, Lafouge F, Boutet-Mercey S, Zoufan P, Sakakibara H, Daniel-Vedele F, Krapp A. 2014. The Arabidopsis nitrate transporter NRT2.5 plays a role in nitrate acquisition and remobilization in nitrogen-starved plants. The Plant Journal: For Cell and Molecular Biology **80**, 230–241.

Liu Q, Wu K, Song W, Zhong N, Wu Y, Fu X. 2022. Improving Crop Nitrogen Use Efficiency Toward Sustainable Green Revolution. Annual Review of Plant Biology **73**, 523–551.

Lu Y-T, Liu D-F, Wen T-T, Fang Z-J, Chen S-Y, Li H, Gong J-M. 2022. Vacuolar nitrate efflux requires multiple functional redundant nitrate transporter in Arabidopsis thaliana. Frontiers in Plant Science **13**, 926809.

Matt P, Geiger M, Walch-Liu P, Engels C, Krapp A, Stitt M. 2001. The immediate cause of the diurnal changes of nitrogen metabolism in leaves of nitrate-replete tobacco: a major imbalance between the rate of nitrate reduction and the rates of nitrate uptake and ammonium metabolism during the first part of the light period. Plant, Cell & Environment **24**, 177–190.

McIntyre GI. 1997. The role of nitrate in the osmotic and nutritional control of plant development. Australian Journal of Plant Physiology **24**, 103–118.

Melino VJ, Tester MA, Okamoto M. 2022. Strategies for engineering improved nitrogen use efficiency in crop plants via redistribution and recycling of organic nitrogen. Current Opinion in Biotechnology **73**, 263–269.

Miller AJ, Fan X, Orsel M, Smith SJ, Wells DM. 2007. Nitrate transport and signalling. Journal of Experimental Botany **58**, 2297–2306.

Miranda KM, Espey MG, Wink DA. 2001. A rapid, simple spectrophotometric method for simultaneous detection of nitrate and nitrite. Nitric Oxide: Biology and Chemistry **5**, 62–71.

Monachello D, Allot M, Oliva S, Krapp A, Daniel-Vedele F, Barbier-Brygoo H, Ephritikhine G. 2009. Two anion transporters AtClCa and AtClCe fulfil interconnecting but not redundant roles in nitrate assimilation pathways. The New Phytologist **183**, 88–94.

737 **Neher E**. 1992. Correction for liquid junction potentials in patch clamp experiments. Ion
738 Channels. Methods in Enzymology. Academic Press, 123–131.

739 **Okamoto M, Vidmar JJ, Glass ADM**. 2003. Regulation of NRT1 and NRT2 gene families of
740 Arabidopsis thaliana: responses to nitrate provision. Plant & Cell Physiology **44**, 304–317.

741 **Orsel M, Eulenburg K, Krapp A, Daniel-Vedele F**. 2004. Disruption of the nitrate transporter
742 genes AtNRT2.1 and AtNRT2.2 restricts growth at low external nitrate concentration. Planta
743 **219**, 714–721.

744 **Orsel M, Filleur S, Fraisier V, Daniel-Vedele F**. 2002. Nitrate transport in plants: which gene
745 and which control? Journal of Experimental Botany **53**, 825–833.

746 **Ow DW, Jacobs JD, Howell SH**. 1987. Functional regions of the cauliflower mosaic virus 35S
747 RNA promoter determined by use of the firefly luciferase gene as a reporter of promoter
748 activity. Proceedings of the National Academy of Sciences of the United States of America **84**,
749 4870–4874.

750 **Schulze W, Schulze E-D, Stadler J, Heilmeier H, Stitt M, Mooney H a.** 1994. Growth and
751 reproduction of Arabidopsis thaliana in relation to storage of starch and nitrate in the wild-
752 type and in starch-deficient and nitrate-uptake-deficient mutants. Plant, Cell & Environment
753 **17**, 795–809.

754 **Shi Y, Liu D, He Y, Tang J, Chen H, Gong P, Luo J-S, Zhang Z**. 2023. CHLORIDE CHANNEL-b
755 mediates vacuolar nitrate efflux to improve low nitrogen adaptation in Arabidopsis. Plant
756 Physiology, kiad438.

757 **Shimada T, Takagi J, Ichino T, Shirakawa M, Hara-Nishimura I**. 2018. Plant Vacuoles. Annual
758 Review of Plant Biology **69**, 123–145.

759 **Wang W, Hu B, Yuan D, *et al.*** 2018. Expression of the Nitrate Transporter Gene
760 OsNRT1.1A/OsNPF6.3 Confers High Yield and Early Maturation in Rice. The Plant Cell **30**, 638–
761 651.

762 **Wege S, De Angeli A, Droillard M-J, *et al.*** 2014. Phosphorylation of the vacuolar anion
763 exchanger AtCLCa is required for the stomatal response to abscisic acid. Science Signaling **7**,
764 ra65.

765 **Wege S, Jossier M, Filleur S, Thomine S, Barbier-Brygoo H, Gambale F, De Angeli A**. 2010. The
766 proline 160 in the selectivity filter of the Arabidopsis NO(3)(-)/H(+) exchanger AtCLCa is
767 essential for nitrate accumulation in planta. The Plant Journal: For Cell and Molecular Biology
768 **63**, 861–869.

769 **Zheng Z-L**. 2009. Carbon and nitrogen nutrient balance signaling in plants. Plant Signaling &
770 Behavior **4**, 584–591.

771

772

775 **Figure legends**

776 **Fig. 1.** Growth effect of *NRT2.7* overexpression in *clca-2* and wild-type backgrounds.
777 (A) Pictures of wild type (WS), *clca-2*, complemented line (*CLCa-Ox* (*clca-2*)) and
778 *NRT2.7* over-expressing line in *clca-2* (*NRT2.7-Ox* (*clca-2*)) on the left side and, WS
779 and the two *NRT2.7* over-expressing lines, *NRT2.7-Ox1* (WS) and *NRT2.7-Ox2* (WS)
780 on the right side. Plants were grown on 2 mM nitrate for 12 days (Scale bars=1 cm).
781 Shoot fresh weight (B) and total root length (C) were measured on wild type (WS), *clca-*
782 *2*, *CLCa-Ox* (*clca-2*) and *NRT2.7-Ox* (*clca-2*) (left side of the panel) or WS, *NRT2.7-*
783 *Ox1* (WS) and *NRT2.7-Ox2* (WS) (right side of the panel). The number of samples
784 were 4-5 for shoot fresh weight (one sample = a pool of 3-4 plants) and n=15-17 for
785 total root length on individual plants. One representative experiment out of three is
786 shown. The numbers above the bars showed the percentage increase or decrease
787 compared to WS. Presented data are means ± Standard Error of the Mean (SEM).
788 Different letters at the top of the bars represent significant difference (p value<0.05).

789 **Fig. 2.** Nitrate content of *NRT2.7* overexpression in *clca-2* and wild-type backgrounds.
790 Wild type (WS), *clca-2*, complemented line (*CLCa-Ox* (*clca-2*)) and *NRT2.7* over-
791 expressing line in *clca-2* (*NRT2.7-Ox* (*clca-2*)) (A, C) or WS and the two *NRT2.7* over-
792 expressing lines, *NRT2.7-Ox1* (WS) and *NRT2.7-Ox2* (WS) (B, D), were grown on 2
793 mM nitrate. After 12 days on the medium, shoot (A, B) and root (C, D) nitrate contents
794 were measured. Two to three biological replicates were performed on each genotype,
795 one sample corresponding to a pool of at least 50 plants. One representative
796 experiment out of two is shown. The numbers above the bars showed the percentage
797 increase or decrease compared to WS. Presented data are means ± SEM. Different
798 letters at the top of the bars represent significant difference (p value<0.05).

799 **Fig. 3.** Effect of *NRT2.7* overexpression in *clca-2* and wild-type backgrounds on nitrate
800 uptake activities. Wild type (WS), *clca-2*, complemented line (*CLCa-Ox* (*clca-2*)),
801 *NRT2.7* over-expressing line in *clca-2* (*NRT2.7-Ox* (*clca-2*)) and the two *NRT2.7* over-
802 expressing lines, *NRT2.7-Ox1* (WS) and *NRT2.7-Ox2* (WS), were grown on vertical
803 Petri dishes on a medium containing 2 mM nitrate for 12 days. Uptake experiments
804 consisted of four to five measurements of $^{15}NO_3^-$ in roots from seedling that were
805 incubated for 5 min in a liquid medium containing 6 mM (A = HATS+LATS) or 0.2 mM
806 (B = HATS) $^{15}NO_3^-$. The activity of LATS (C) was obtained by subtracting the activity
807 measured at 0.2 mM to the one at 6 mM (see material and methods section for details).

808 Presented data are averages of three independent experiments (n=3-5 by independent
809 experiment). Bars represents means ± SEM. The numbers above the bars showed the
810 percentage increase or decrease compared to WS. Different letters at the top of the
811 bars represent significant difference (p value<0.05).

812 **Fig. 4.** Effect of limiting N supply on the phenotype of *NRT2.7* over-expressers. Wild
813 type (WS) and over-expressing lines, *NRT2.7-Ox1* (WS) and *NRT2.7-Ox2* (WS), were
814 grown in petri dishes for 12 days on 0.2 mM nitrate. Shoot fresh weight (A), total root
815 length (B) shoot and root nitrate contents (C, D) were measured as described in Figure
816 1 and 2. C/N ratios, percentages of N and C contents were measured in shoot (E) and
817 root (F) using an elementary analyser. Data are averages of four biological replicates
818 for shoot fresh weight, 12 to 17 for total root length, two to four for nitrate contents and
819 four for C and N contents. The numbers above the bars showed the percentage
820 increase or decrease compared to WS. Different letters show significant differences
821 between genotypes (p<0.05).

822 **Fig. 5.** Nitrate efflux from mesophyll vacuoles is increased in *NRT2.7-Ox* (*clca-2*) plants
823 compared to *clca-2* knock-outs. (A) Representative whole-vacuole currents measured
824 in vacuoles extracted from *clca-2* knock-out mutant (left) and *NRT2.7-Ox* (*clca-2*)
825 transgenic line (right) in presence of nitrate only in the vacuolar lumen (200 mM NO_3^-
826 pH 5.5 in the vacuolar buffer, 19.2 mM Cl^- in the cytosolic buffer, see Materials and
827 Methods). Currents were evoked in response to 2 s voltage pulses ranging from -77
828 mV to +83 mV in +20 mV steps, followed by a tail pulse at +33 mV, with a holding
829 potential at -17 mV. (B) Box plot of the mean current density (pA/pF) measured at
830 different positive (left) and negative (right) membrane potentials in vacuoles from
831 *NRT2.7-Ox* (*clca-2*) (vertical diamonds line *NRT2.7-Ox1* (*clca-2*), n=11; horizontal
832 diamonds line *NRT2.7-Ox2* (*clca-2*), n=5), and *clca-2* knock-out plants, n=10. The ionic
833 conditions were as in (A). Boxes defines the first and the third quartile and the median,
834 the whiskers represent the ninth and the ninety-first percentiles. The two asterisks
835 indicate a statistical significance at 1% level with a Mann-Whitney test.

836

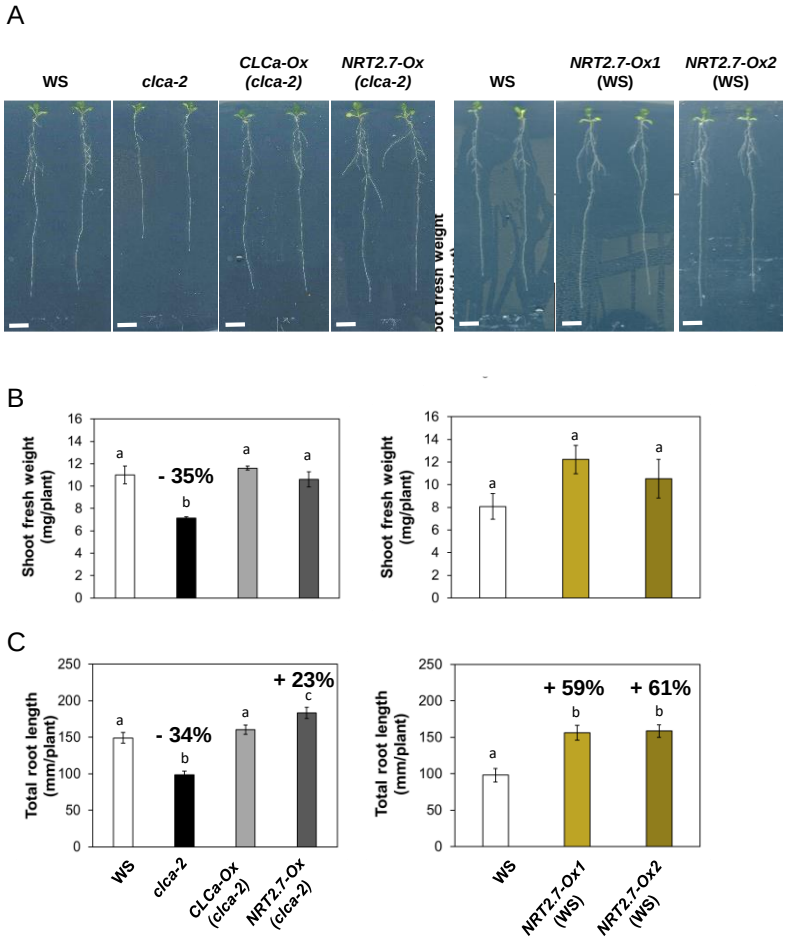

Fig. 1. Growth effect of *NRT2.7* overexpression in *clca-2* and wild-type backgrounds. (A) Pictures of wild type (WS), *clca-2*, complemented line (*CLCa-Ox* (*clca-2*)) and *NRT2.7* over-expressing line in *clca-2* (*NRT2.7-Ox* (*clca-2*)) on the left side and, WS and the two *NRT2.7* over-expressing lines, *NRT2.7-Ox1* (WS) and *NRT2.7-Ox2* (WS) on the right side. Plants were grown on 2 mM nitrate for 12 days (Scale bars=1 cm). Shoot fresh weight (B) and total root length (C) were measured on wild type (WS), *clca-2*, *CLCa-Ox* (*clca-2*) and *NRT2.7-Ox* (*clca-2*) (left side of the panel) or WS, *NRT2.7-Ox1* (WS) and *NRT2.7-Ox2* (WS) (right side of the panel). The number of samples were 4-5 for shoot fresh weight (one sample = a pool of 3-4 plants) and n=15-17 for total root length on individual plants. One representative experiment out of three is shown. The numbers above the bars showed the percentage increase or decrease compared to WS. Presented data are means ± Standard Error of the Mean (SEM). Different letters at the top of the bars represent significant difference (p value<0.05).

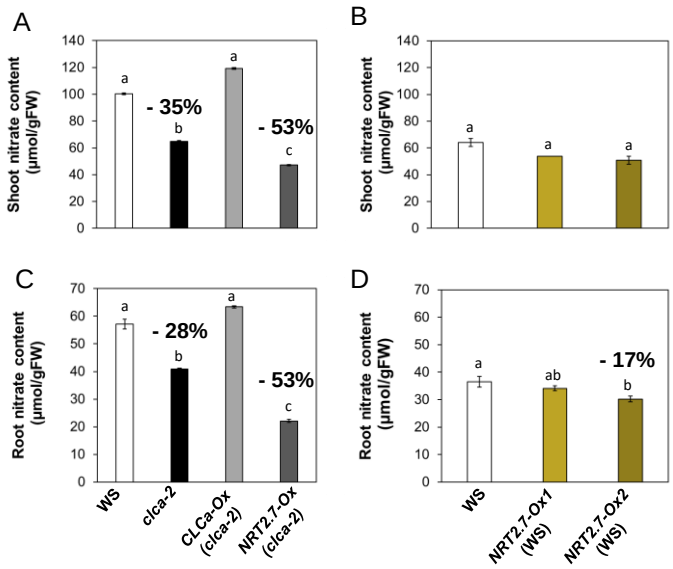

Fig. 2. Nitrate content of *NRT2.7* overexpression in *clca-2* and wild-type backgrounds. Wild type (WS), *clca-2*, complemented line (*CLCa-Ox* (*clca-2*)) and *NRT2.7* over-expressing line in *clca-2* (*NRT2.7-Ox* (*clca-2*)) (A, C) or WS and the two *NRT2.7* over-expressing lines, *NRT2.7-Ox1* (WS) and *NRT2.7-Ox2* (WS) (B, D), were grown on 2 mM nitrate. After 12 days on the medium, shoot (A, B) and root (C, D) nitrate contents were measured. Two to three biological replicates were performed on each genotype, one sample corresponding to a pool of at least 50 plants. One representative experiment out of two is shown. The numbers above the bars showed the percentage increase or decrease compared to WS. Presented data are means ± SEM. Different letters at the top of the bars represent significant difference (p value<0.05).

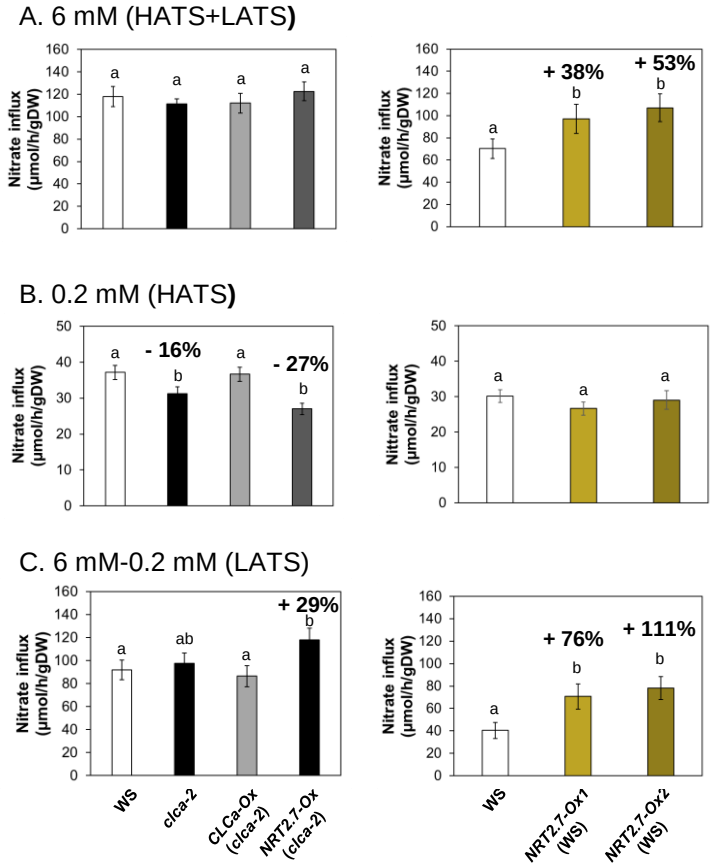

Fig. 3. Effect of *NRT2.7* overexpression in *clca-2* and wild-type backgrounds on nitrate uptake activities. Wild type (WS), *clca-2*, complemented line (*CLCa-Ox* (*clca-2*)), *NRT2.7* over-expressing line in *clca-2* (*NRT2.7-Ox* (*clca-2*)) and the two *NRT2.7* over-expressing lines, *NRT2.7-Ox1* (WS) and *NRT2.7-Ox2* (WS), were grown on vertical Petri dishes on a medium containing 2 mM nitrate for 12 days. Uptake experiments consisted of four to five measurements of $^{15}NO_3^-$ in roots from seedling that were incubated for 5 min in a liquid medium containing 6 mM (A = HATS+LATS) or 0.2 mM (B = HATS) $^{15}NO_3^-$. The activity of LATS (C) was obtained by subtracting the activity measured at 0.2 mM to the one at 6 mM (see material and methods section for details). Presented data are averages of three independent experiments (n=3-5 by independent experiment). Bars represents means ± SEM. The numbers above the bars showed the percentage increase or decrease compared to WS. Different letters at the top of the bars represent significant difference (p value<0.05).

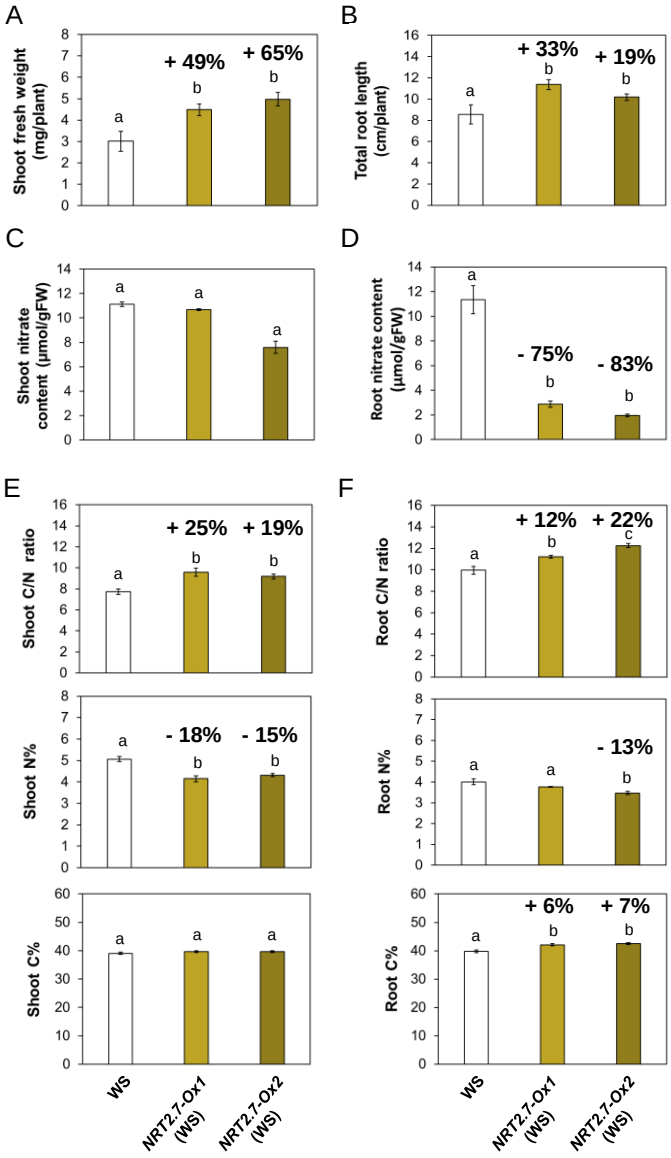

Fig. 4. Effect of limiting N supply on the phenotype of *NRT2.7* over-expressers. Wild type (WS) and over-expressing lines, *NRT2.7-Ox1* (WS) and *NRT2.7-Ox2* (WS), were grown in petri dishes for 12 days on 0.2 mM nitrate. Shoot fresh weight (A), total root length (B) shoot and root nitrate contents (C, D) were measured as described in Figure 1 and 2. C/N ratios, percentages of N and C contents, were measured in shoot (E) and root (F) using an elementary analyser. Data are averages of two to four measurements, except for B, n=12-17 (bars representing the SEM). The numbers above the bars showed the percentage increase or decrease compared to WS. Different letters show significant differences between genotypes ($p<0.05$).

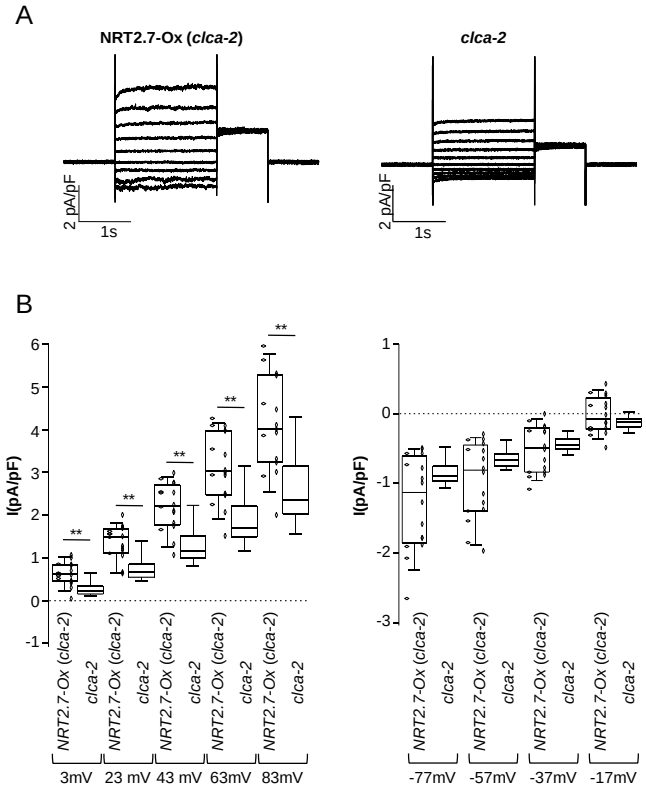

Fig. 5. Nitrate efflux from mesophyll vacuoles is increased in *NRT2.7-Ox* (*clca-2*) plants compared to *clca-2* knock-outs. (A) Representative whole-vacuole currents measured in vacuoles extracted from *clca-2* knock-out mutant (left) and *NRT2.7-Ox* (*clca-2*) transgenic line (right) in presence of nitrate only in the vacuolar lumen (200 mM NO_3^- pH 5.5 in the vacuolar buffer, 19.2 mM Cl^- in the cytosolic buffer, see Materials and Methods). Currents were evoked in response to 2 s voltage pulses ranging from -77 mV to +83 mV in +20 mV steps, followed by a tail pulse at +33 mV, with a holding potential at -17 mV. (B) Box plot of the mean current density (pA/pF) measured at different positive (left) and negative (right) membrane potentials in vacuoles from *NRT2.7-Ox* (*clca-2*) (vertical diamonds line *NRT2.7-Ox1* (*clca-2*), n=11; horizontal diamonds line *NRT2.7-Ox2* (*clca-2*), n=5), and *clca-2* knock-out plants, n=10. The ionic conditions were as in (A). Boxes defines the first and the third quartile and the median, the whiskers represent the ninth and the ninety-first percentiles. The two asterisks indicate a statistical significance at 1% level with a Mann-Whitney test.

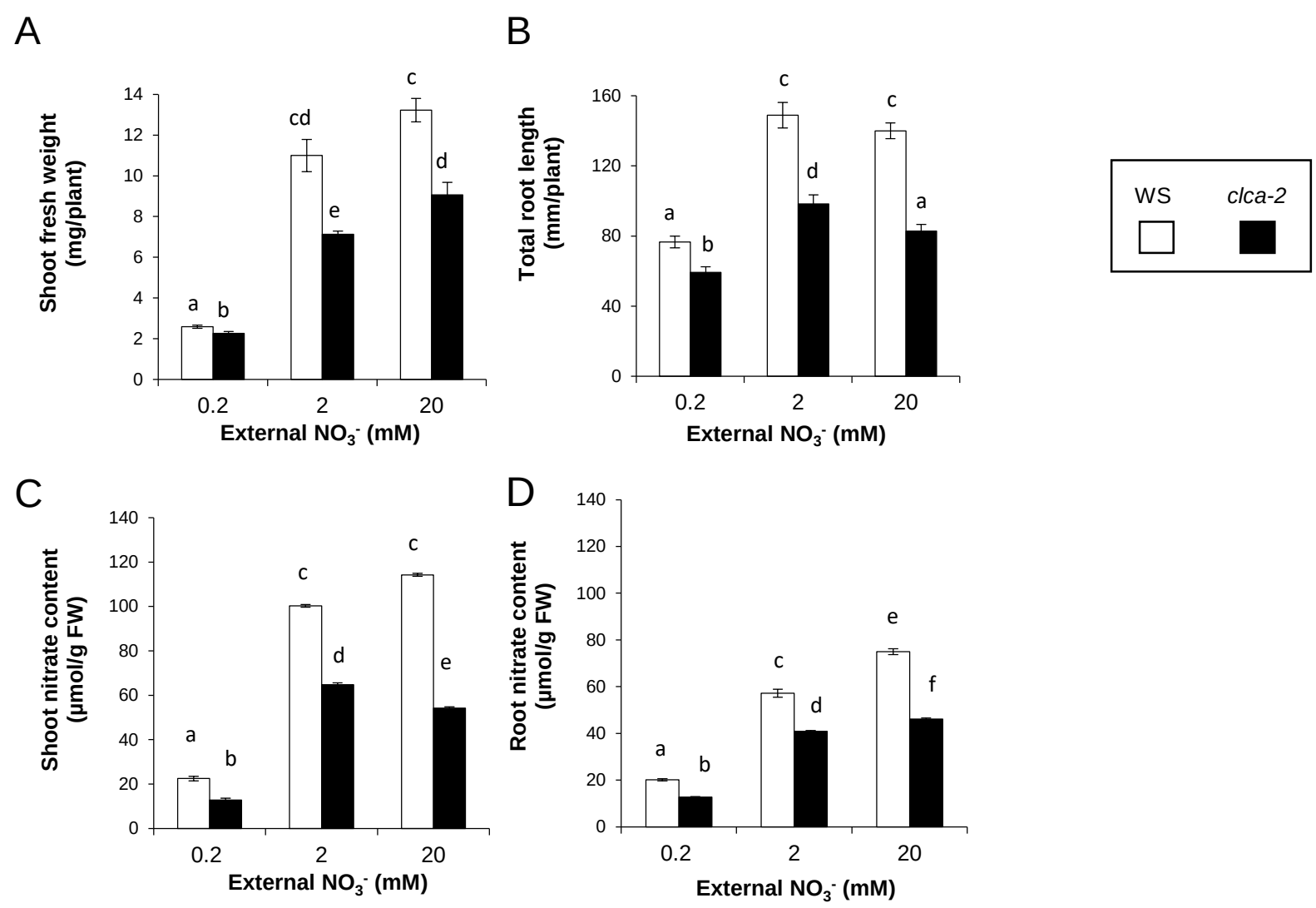

Supplementary Fig. S1. *clca-2* knock-out mutant phenotype. Wild-type (WS) and *clca-2 p*lants were grown on vertical Petri dishes for 12 days on 0.2, 2 or 20 mM external nitrate as described in the 'Materials and Methods'. Shoot fresh weight (A), total root length (B), shoot and root nitrate contents (C and D) were measured in WS (white boxes) and *clca-2* (black boxes) after 12 days of growth (A). Data are means ± SEM of 4-5 (A) or 16-20 measurements (B). For nitrate measurements, data are means ± SEM of three technical replicates of a representative experiment. Each point is a pool of at least 50 plants. Different letters at the top of the bars represent significant difference (p value<0.05).

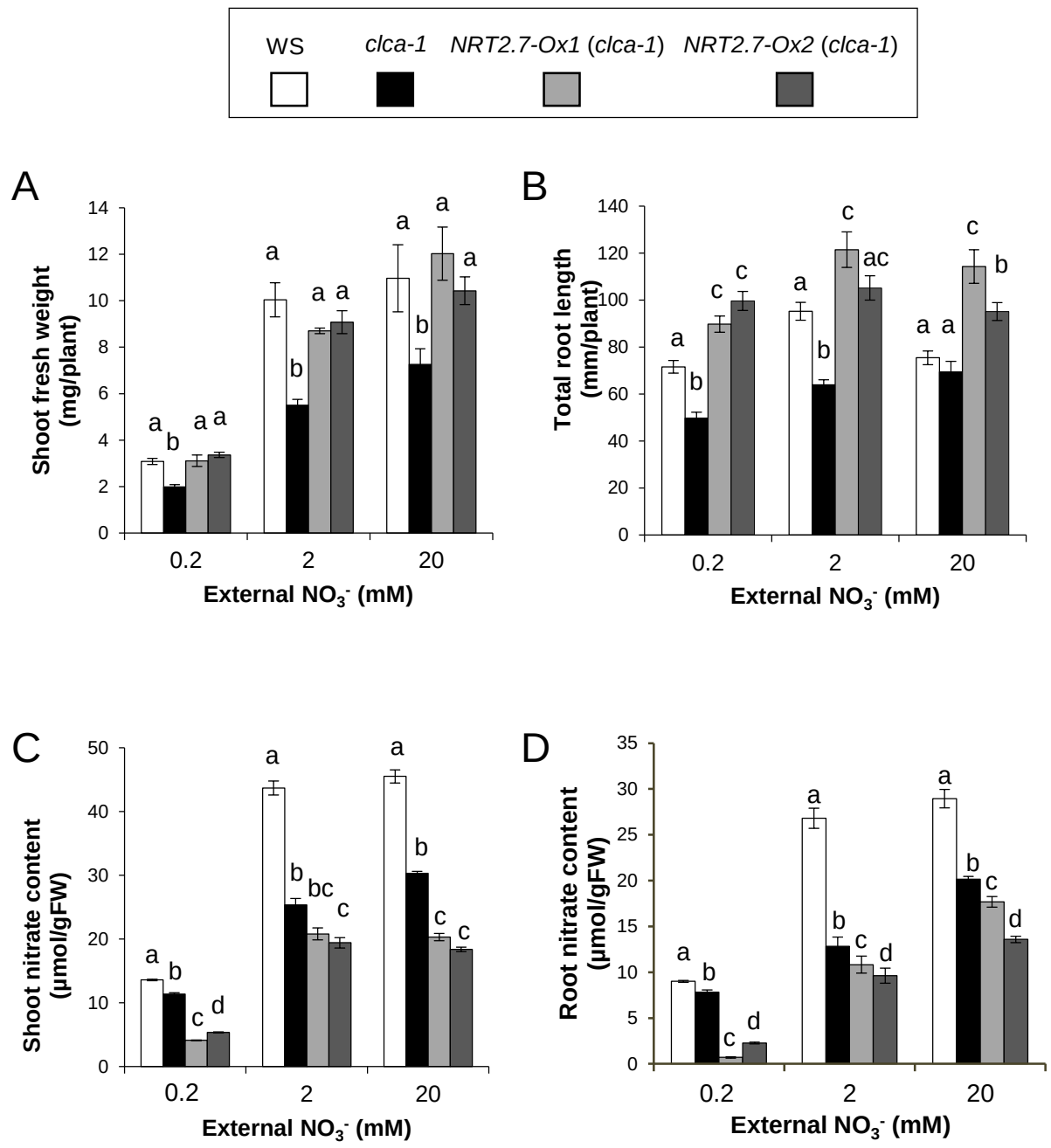

Supplementary Fig. S2. Growth and nitrate content of *NRT2.7* overexpressors in the c*lca-1* knock-out mutant backgound. Wild type (WS), *clca-1* and two over-expressing lines, *NRT2.7-Ox1* (*clca-1*) and *NRT2.7-Ox2* (*clca-1*) were grown on vertical Petri dishes for 12 days on 0.2, 2 or 20 mM external nitrate as described in the 'Materials and Methods'. Shoot fresh weight was measured after 12 days of growth (A), and total root length were analyzed on 9 day-old plant (B). Data are averages of 4-5 (A) or 11-20 measurements (B). Shoot (C) and root (D) nitrate content in 12 day-old plants. Data are averages of three technical nitrate measurements of a representative experiment. Each point is a pool of at least 50 plants. Vertical bars represent means ± SEM. Different letters at the top of the bars represent significant difference (p value<0.05).

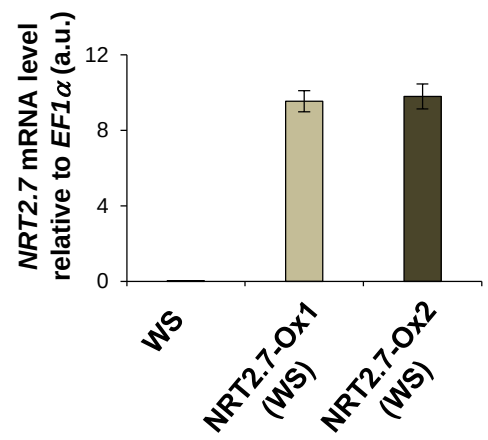

Supplementary Fig. S3. Level of *NRT2.7* expression in *NRT2.7-Ox* (WS). Plants were grown on vertical Petri dishes for 12 days on 2 mM external nitrate as described in the 'Materials and Methods'. RT-qPCR was performed on total RNA extracted from shoot using *NRT2.7* and *EF1α* specific primers. Data represents the means ± SEM of three biological replicates.

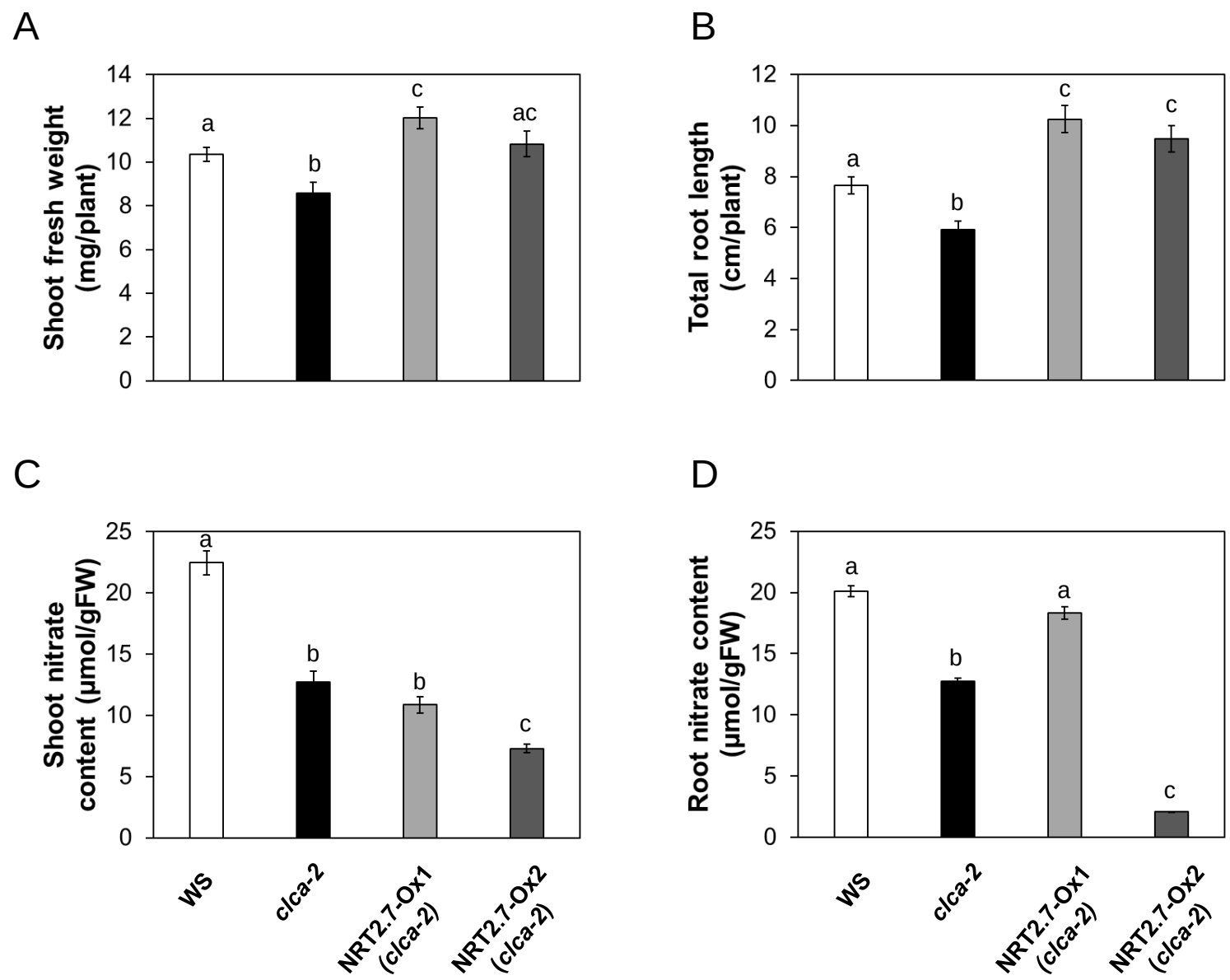

Supplementary Fig. S4. Effect of limiting N supply on the phenotype of *NRT2.7* over-expressors in *clca-2* background. Wild type (WS), *clca-2,* complemented line (*CLCa-Ox* (*clca-2*)) and *NRT2.7* over-expressing line in *clca-2* (*NRT2.7-Ox* (*clca-2*)) were grown in petri dishes for 12 days on 0.2 mM nitrate. Shoot fresh weight (A), total root length (B) and, shoot and root nitrate contents (C, D) were measured as described in Figure 1 and 2. Data are averages of three to five measurements, except for B, n=12-19 (bars representing the SEM). Different letters show significant differences between genotypes ($p<0.05$).

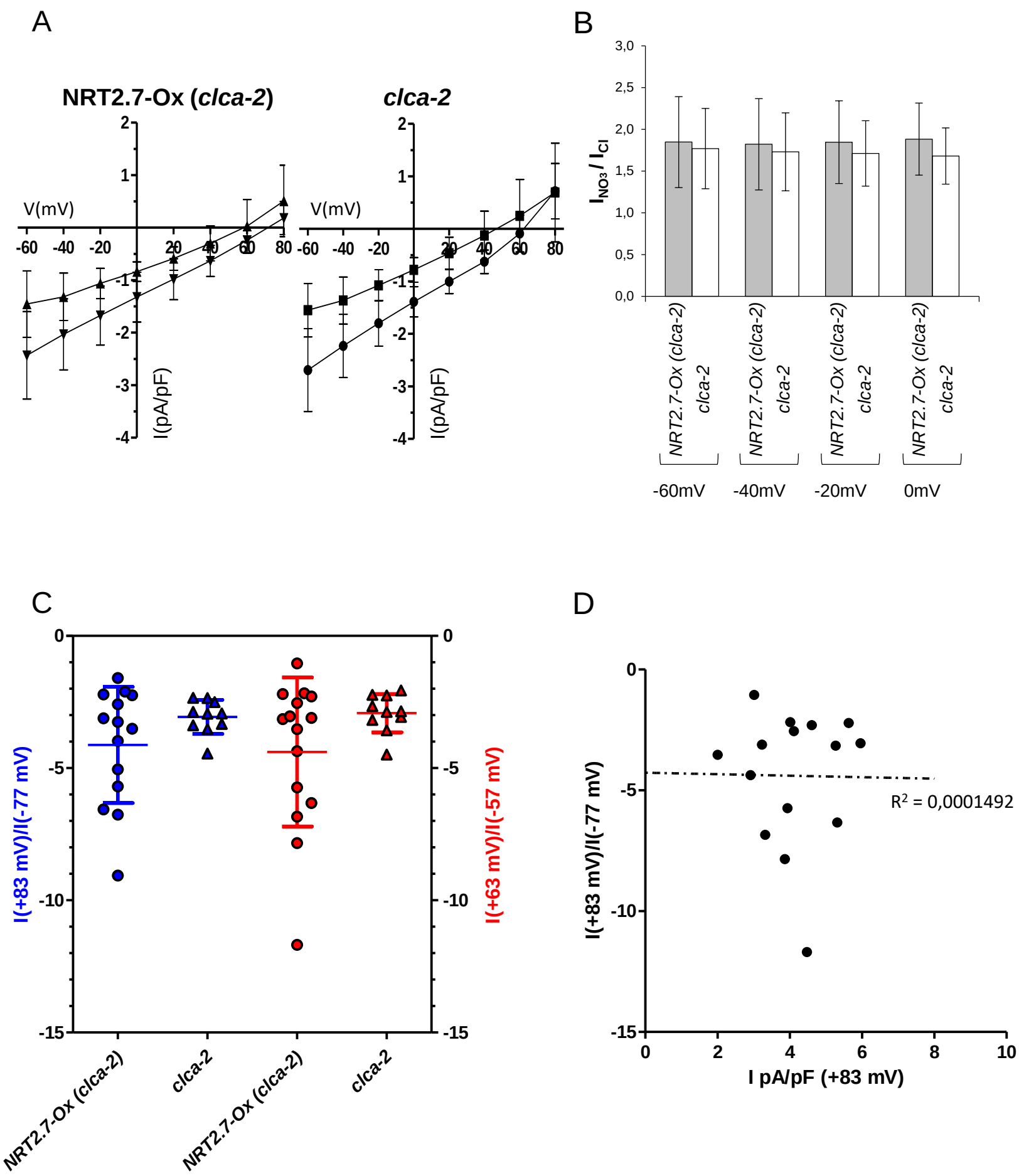

Supplementary Fig. S5. Nitrate influx is not increased in vacuoles from *NRT2.7_Ox* (*clca2*) expressing plants compared to vacuoles of *clca-2* knock-outs. (A) mean IV curves measured in vacuoles extracted from NRT2.7-Ox (*clca-2*) (top, n=6) and *clca-2* knock-out (bottom, n=6) without nitrate in the vacuolar lumen (15 mM Cl^-, pH=5.7, see Materials and methods) and in absence (square) and presence (circle) of cytosolic nitrate (4 mM NO_3^- pH=7). (B) current ratio (I_{NO3}^-/I_{cl}^-) calculated from cytosolic solution exchange experiments at different membrane potentials. Error bars are standard deviation. (C) Rectification rates calculated as I(+83mV)/I(-77mV) (blue, left axis) and I(+63mV)/I(-57mV) (red, right axis). The Rectification rate was calculated from the individual vacuoles extracted from *clca-2* knock-out mutant (triangles) and *NRT2.7-Ox* (*clca-2*) transgenic line (circles) shown in Fig. 5. Ionic currents were recorded in presence of nitrate only in the vacuolar lumen (200 mM NO_3^- pH 5.5 in the vacuolar buffer, 19.2 mM Cl^- in the cytosolic buffer, see Materials and Methods). Statistical significance between *clca-2* knock-out mutant (triangles) and *NRT2.7-Ox* (*clca-2*) transgenic line (circles) was calculated with a non-parametrical Mann-Whitney test. (D) Plot showing the rectification rate I(+83mV)/I(-77mV) (blue, left axis) vs the current density of each vacuole of the *NRT2.7-Ox* (*clca-2*) transgenic line. The broken line shows a liner regression fit of the data illustrating the absence of correlation between the current intensity recorded in each vacuole and the rectification.